Bioactive Materials 5 (2020) 871–879

Contents lists available at ScienceDirect

Bioactive Materials

journal homepage: http://www.keaipublishing.com/biomat

Injectable ECM hydrogel for delivery of BMSCs enabled full-thickness meniscus repair in an orthotopic rat model

Gang Zhong[a,b,1], Jun Yao[b,1], Xing Huang[b], Yixuan Luo[a], Meng Wang[a], Jinyu Han[a], Fei Chen[a,*], Yin Yu[a,**]

[a] Center for Materials Synthetic Biology, CAS Key Laboratory of Quantitative Engineering Biology, Shenzhen Institute of Synthetic Biology, Shenzhen Institutes of Advanced Technology, Chinese Academy of Sciences, Shenzhen, 518055, China
[b] Department of Orthopedics Trauma and Hand Surgery & Guangxi Key Laboratory of Regenerative Medicine, International Joint Laboratory on Regeneration of Bone and Soft Tissue, The First Affiliated Hospital of Guangxi Medical University, Nanning, China

ARTICLE INFO

Keywords:
Meniscus derived extracellular matrix
Bone marrow stromal cells
Meniscal tissue engineering
Hydrogels

ABSTRACT

Meniscal injuries have poor intrinsic healing capability and are associated with the development of osteoarthritis. Decellularized meniscus extracellular matrix (mECM) has been suggested to be efficacious for the repair of meniscus defect. However, main efforts to date have been focused on the concentration, crosslinking density and anatomical region dependence of the mECM hydrogels on regulation of proliferation and differentiation of adult mesenchymal stem cells (MSCs) *in vitro* 2D or 3D culture. A systematic investigation and understanding of the effect of mECM on encapsulated MSCs response and integrative meniscus repair by *in vivo* rat subcutaneous implantation and orthotopic meniscus injury model will be highly valuable to explore its potential for clinical translation. In this study, we investigated the *in situ* delivery of rat BMSCs in an injectable mECM hydrogel to a meniscal defect in a SD rat model. Decellularized mECM retained essential proteoglycans and collagens, and significantly upregulated expression of fibrochondrogenic markers by BMSCs versus collagen hydrogel alone *in vitro* 3D cell culture. When applied to an orthotopic model of meniscal injury in SD rat, mECM is superior than collagen I scaffold in reduction of osteophyte formation and prevention of joint space narrowing and osteoarthritis development as evidenced by histology and micro-CT analysis. Taken together, these results indicate mECM hydrogel is a highly promising carrier to deliver MSCs for long-term repair of meniscus tissue, while preventing the development of osteoarthritis.

1. Introduction

Meniscus plays an important role in maintaining the stability of joints and conducting mechanical loads [1]. Meniscal injuries are a common and important cause of knee dysfunction [2]. Indulgence will lead to severe joint degeneration and mineral loss. Unfortunately, meniscus injuries, especially those in the avascular inner zone have a poor healing capability [3]. Currently, partial meniscectomy is commonly practiced to reduce pain and mechanical symptoms, despite knowing that partial removal of meniscal tissue contributes to the development of OA [4].

In this regard, tissue engineering approaches that use biomaterial scaffolds in combination with potential therapeutic cells provide a novel approach for functional repair of meniscal injuries [5]. In particular, meniscus derived ECM has been shown to promote injured meniscus tissue remodeling and integrative repair by providing abundance of native biochemical components and growth factors [6].

Several prior studies have generated meniscus tissue-derived scaffolds for either tissue repair or replacement. Whole meniscus tissue has been decellularized to generate allograft scaffold for meniscus repair. However, the dense ECM limits cellular migration into the allografts, a process that is necessary for long-term regeneration and repair [7]. In addition, previous studies have mostly introduced exogenous cytokines such as TGF-β3 [8,9], BMP2 [10] and EGFR [11]into the hydrogel, which not only interfered with our judgment of the intrinsic potential of the scaffold, but also greatly limited the clinical translation in regard to

Peer review under responsibility of KeAi Communications Co., Ltd.
* Corresponding author.,
** Corresponding author.
E-mail addresses: fei.chen1@siat.ac.cn (F. Chen), yin.yu@siat.ac.cn (Y. Yu).
[1] These authors contributed equally to this work.

https://doi.org/10.1016/j.bioactmat.2020.06.008
Received 30 March 2020; Received in revised form 12 June 2020; Accepted 12 June 2020

regulatory paths. Other studies have used physical disruption [12], enzymatic treatments [13], chemical treatments or a combination therefore to generate porous scaffold or hydrogels [9] to promote endogenous cell migration. While many previous studies investigated the effect of mECM concentration and various methods of crosslinking on scaffold integrity enhancement and the exogenous meniscus cellular response in a meniscus repair model system *in vitro* [14–16] or *ex vivo* [17], there has been little examination of the long-term efficacy of mECM in pertinent animal models for meniscus repair.

Thus, the aim of this study was to compare the effect of mECM with Collagen I from bovine skin in promoting chondrogenic/fibrochondrogenic differentiation of encapsulated BMSCs and long-term efficacy of these scaffold in an orthotopic SD rat meniscal injury model. For this purpose, we processed the inner region of porcine meniscus into an injectable hydrogel solution via modified decellularization and enzymatic digestion. BMSCs were first encapsulated in Collagen I or mECM hydrogel then injected to the meniscus defect through an arthroscopic meniscectomy surgery. The extent of decellularization and cellular response in 3D culture were evaluated *in vitro*. Finally, a subcutaneous implantation model and an orthotopic SD rat meniscal injury model were used to evaluate the effect of both scaffold for functional meniscus repair and preventative effect of osteoarthritis development.

2. Materials and methods

2.1. Decellularization and digestion of porcine meniscus extracellular matrix

Meniscus tissues were harvested from the hindleg stifle of 6 to 7-month-old porcine knee joints which were purchased from pork retailer within 12 h of slaughter. The preparation of meniscus-derived extracellular matrix (mECM) was carried out as described previously [18]. One third of the medial meniscus samples was preserved and washed with PBS and then cut into small chips with size of 5–10 mm^3. Meniscal chips were expanded with acetic acid solution (0.01 M, pH 2) for 48 h at 4 °C and were performed three cycles of freeze–thaw by freezing the samples at −80 °C for 24h then leaving the tissue to thaw at room temperature for 4h. Samples were decellularized in 2% SDS and 10 mM Tris at 25 °C with agitation (3 cycles, 24 h each), followed by 0.1% peracetic acid (2 h), washed in sterile water and PBS with aprotinin for 12h with agitation (3 cycles), and lyophilized again (24 h). The resulting sponge-like mECM was digested in 0.1% pepsin +0.01 M HCl (pH 2) at a concentration of 50 mg/mL at 25 °C with agitation (12 h), resulting in a mECM digest solution. Then, the decellularized ECM was treated with 200 U/mL DNase (Thermo Fisher Scientific, USA) and 50 U/mL RNase (Thermo Fisher Scientific, USA) solution at 37 °C for 24 h and then washed in PBS (6 cycles, 30 min each). Efficient removal of DNA was confirmed by the lack of cell nuclei using 4′, 6-diamidino-2-phenylindole (DAPI, Thermo Fisher Scientific, USA) staining and by a reduction in the double-stranded DNA content using PicoGreen dsDNA Quantitation Kits (Invitrogen, USA), compared with that of native meniscus tissues. Collagen [19], GAGs content [20] retention was confirmed by biochemical analysis. Before use, adjust the pH of mECM solution to neutral using 0.5 mol/L NaOH solution and then adjust the concentration to 3 mg/mL using 1 x PBS and store it at 4 °C.

2.2. Culture of rat bone marrow derived stem cells (BMSCs)

BMSCs were isolated from rat bone marrow aspirates as described in a previous work [21]. Briefly, bone marrow was collected from femurs by inserting a 22-gauge needle into the shaft of the femur and flushed with 3 mL PBS (Sigma, USA). BMSCs were cultured in complete growth medium (alpha-modified eagle's medium (αMEM, GIBCO, USA), 10% fetal bovine serum (Sigma, USA), 100 U/mL penicillin and 100 mg/mL streptomycin) at 37 °C and 5.0% CO_2 in a humidified incubator. The culture medium was replaced every 3 days. All experiments were performed with BMSCs at passage 3.

2.3. Encapsulation of BMSCs in mECM or hydrogel

Collagen I (PureCol®, Advanced BioMatrix, USA) from bovine skin was prepared as previously described [22]. mECM and collagen were neutralized with 0.5 M NaOH and diluted with 1 x PBS to reach final concentration of 0.3 mg/mL and 3 mg/mL and stored at 4 °C respectively before use. BMSCs from SD rat were mixed with neutralized mECM or Cowhide collagen solution by vortex at a concentration of 1×10^7 cells/mL, gelated at 37 °C for 10 min, then cultured in complete media. Samples were collected at days 7, 14, 21 for biochemical, histological and gene expression analyses. Samples were also collected at days 7 for cell viability analysis and at days 21 for SEM and Western Blot analysis (see Supplemental Information).

2.4. In vivo subcutaneous implantation model in SD rat

Male SD rats at 7 weeks of age were anesthetized by intraperitoneal injections of 2% pentobarbital sodium. After 7 days of *in vitro* culture, The BMSCs (1×10^6 cells) encapsulated in mECM (100 μL) were placed into the back of SD rats by surgical operation. In detail, a 1 cm skin incision was made longitudinally on the midline of the back of the rat, then 3D constructs were implanted into separate subcutaneous dorsal pockets (1 construct per pocket, 2 pockets per animal), the skin was sutured carefully, and 80,000 units of penicillin solution were injected intraperitoneally according to an approved protocol at Guangxi Medical University, China. Implants were collected after 4 weeks transplantation and evaluated for histological staining.

2.5. Orthotopic model of meniscal injury in SD rat

The white area of the medial anterior horn of the meniscus of SD rats (n = 18) was made into a full-thickness defect model by microsurgery under the microscope. Briefly, male SD rats at 7 weeks of age were anesthetized with 2% w/v pentobarbital sodium, with analgesia with 10 mg/kg Tramadol. After disinfection, the anterior joint of the rat was exposed by the longitudinal incision of the joint capsule through the medial approach of the patellar ligament with aseptic technique. The anterior horn of the medial meniscus was dislocated anteriorly, resulting in a 0.6-mm-diameter through-hole defect in the meniscus. BMSCs (5×10^5 cells) encapsulated in mECM (30 μL) or Cowhide collagen (30 μL) were injected into the defect by 25-gauge needle. The incision was sutured layer by layer (articular capsule, muscle, subcutaneous tissue, skin) after injection of BMSCs with Cowhide collagen or mECM. Normal saline (n = 6) was injected as a negative control. The rats were placed in a warm box (26 °C), and tramadol 10 mg/kg was used for analgesia 2 h post-surgery. At eight weeks post-injury, all animals were euthanized through CO_2 induction, the joint tissue was exposed and its macroscopic observation was recorded through Huawei mate 9 (Huawei, China). Meniscus tissues were harvested and fixed in 4% paraformaldehyde for 48 h for histological analyses.

2.6. Micro-computed tomography (μCT) analysis of SD rat

All rats were imaged in micro-computed tomographic (μCT) scanner (NEMO micro-CT, PINGSENG Healthcare, China) at four weeks and eight weeks post-surgery. Under anesthesia by 2% pentobarbital sodium, μCT scanning was performed with focus over the hindlimbs with a 90 kVP tube voltage and 80 μA current. 3D segmentation of the CT images was performed by using a commercial image processing software (Recon; PINGSENG, Shanghai, China). Indirect measures of knee joint space volumes (JSV) of each animal at each time point were achieved by calculating the difference between a fixed cubic volume and the bone volume [9].

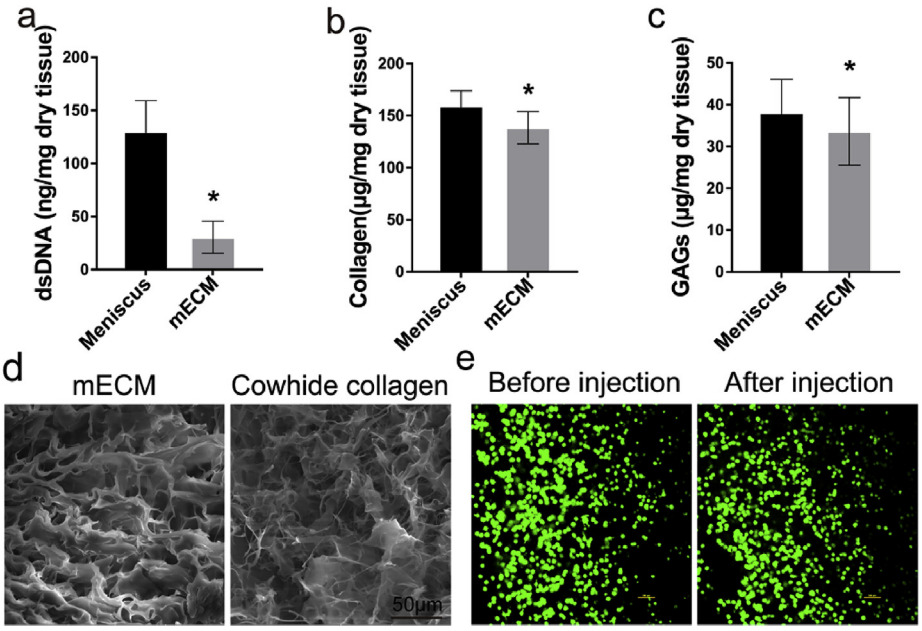

Fig. 1. Characterization of decellularized meniscus scaffolds. (a) dsDNA, (b) collagen, (c) GAGs levels of scaffolds were quantified by biochemical assay. (d) SEM images of mECM and Cowhide collagen scaffolds, Scale bar = 50 μm. (e) Cell viability of BMSCs mixed with mECM before and after extrusion from 25 G needle was assessed by confocal microscopy by live/dead staining (FDA, green; PI, red). Values are presented as means ± SD, n = 5. *, $P < 0.05$; relative to the normal group; Scale bar = 100 μm.

2.7. Gene expression in BMSCs in vitro culture

Cell-laden mECM or Cowhide collagen at days 7, 14, and 21 were homogenized by pellet pestle. Total RNA was extracted in RNA extraction kit (Tiangen Biotech Co., Ltd., China) and digested with DNase to remove any contaminating genomic DNA in accordance with the manufacturer's instructions. First-strand complementary DNA (cDNA) was synthesized using a cDNA synthesis kit (Invitrogen, USA). Quantitative real-time polymerase chain reaction (qRT-PCR) was performed using Fast Start Universal SYBR Green Master (Roche) by quantitative PCR detection system (Realplex 4, Eppendorf Corporation). The samples were then analyzed by comparative Ct quantification (DDCt method). Primers used for meniscus-associated gene expression included those for *Collagen I*, *Collagen II*, and *Aggrecan*. The targets and sequences of primers are shown in Table S1. The expression level of each gene was standardized by GAPDH.

2.8. Biochemical content of hydrogel-encapsulated cells in vitro

The biochemical compositions of the native and decellularized mECM, BMSCs in mECM and Cowhide collagen hydrogels were quantified for DNA, sulfated glycosaminoglycan (GAGs), and total collagen contents. Briefly, samples were rinsed with PBS, minced and digested with proteinase K (60 μg/mL) at 56 °C for 10 h. The content of DNA in 3D constructs was stained by Hoechst 33258 dye and absorbance was measured at 460 nm by using fluorescence spectrophotometer (Bio-Tek Instruments, USA). Calf thymus DNA was used as the standard. Intracellular GAGs secretion was analyzed using 1,9-dimethylmethylene blue assay (DMMB, Sigma, USA) and the absorption at wavelength of 525 nm was recorded on fluorescence spectrophotometer (Bio-Tek Instruments, USA), and chondroitin sulfate (Sigma, USA) was used as a standard. Finally, intracellular GAGs secretion was normalized to the DNA content of the cells and expressed as GAGs/DNA. Collagen content was quantified by measuring total hydroxyproline content using a Hydroxyproline Assay Kit (Sigma aldrich, USA). A hydroxyproline: collagen ratio of 1:7.69 was assumed to determine the collagen content [23].

2.9. Histological analysis

For histological processing, hydrogel-encapsulated BMSCs at days 7, 14, and 21 were fixed with 4% phosphate-buffered paraformaldehyde at 4 °C for 3 h, dehydrated through a graded series of ethanol, embedded in paraffin, sectioned at a thickness of 4 μm with Slicer (RM2125, LEICA, Germany). All sections were stained with hematoxylin–eosin (H&E) staining reagent (Solarbio, USA), Toluidine blue (Solarbio, USA), Alcian blue and immunohistochemistry reagent (ZSGb Bio, China) for Collagen I (Abcam, USA) in strict accordance with standard protocols provided from manufacturer. Neutral resin sealed-slices were prepared for observation and pictures were captured by an Inverted optical microscope (Olympus, Japan).

For *in vivo* study samples, after gradient alcohol dehydration, the knee tissues were embedded in paraffin. The embedded tissues were then cut into 5 μm frontal sagittal sections. Slides of femur and tibia were stained with H&E (Solarbio, China) and Safranin-O fast green (Solarbio, China) [24]. The morphological manifestations of meniscus tissues were observed in a double-blind manner using a microscope (Olympus, Japan).

2.10. Statistical analysis

Statistical analyses of all data (mean ± S.D) were performed using SPSS 64.0 (SPSS Inc., Chicago, Illinois, USA). Comparisons across control and treatment groups were made using one-way analysis of variance (ANOVA) with Tukey's HSD post hoc testing where a p value < 0.05 was considered significant. Sample sizes are indicated in figure legends.

3. Results

3.1. Efficient decellularization of mECM

The decellularization of meniscus tissue resulted in a significant reduction in dsDNA content (Fig. 1a; native vs decellularized: 130.23 ng/mg vs 30.49 ng/mg), without significant changes in GAGs or collagen content (Fig. 1b and c). We also utilized SEM to visualize the physical structure of mECM and Cowhide collagen scaffolds. mECM prepared by expansion of meniscus in acetic acid possessed a loose porous structure with interconnected pores ranged from 10 μm to 40 μm (Fig. 1d), which is believed to facilitate cell infiltration and proliferation. In order to evaluate the effect of extrusion through needle on BMSCs viability, we performed a live/dead assay for cells mixed

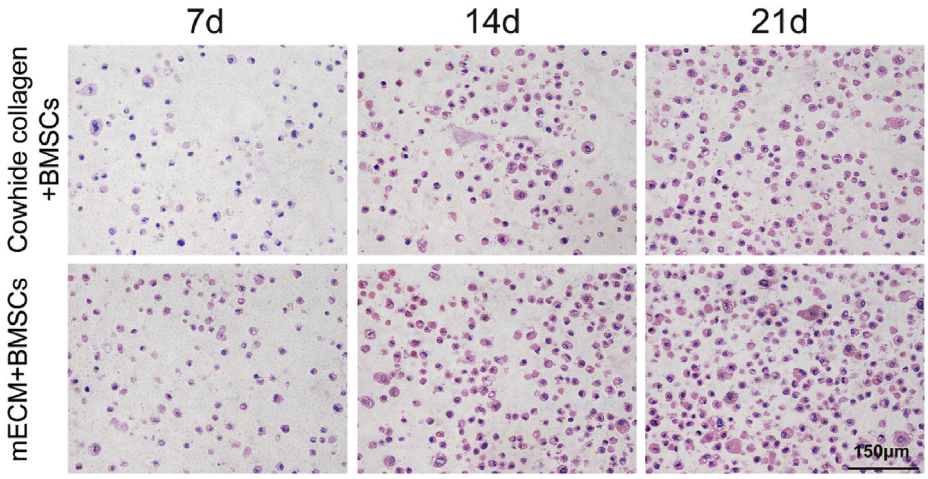

Fig. 2. H&E staining for BMSCs-laden Cowhide collagen and mECM hydrogels over 21 days of culture *in vitro*.

with mECM before and post-extrusion through 25-gauge needle. Fig. 1e shows that BMSCs in mECM maintained high cell viability through the 25-gauge needle before and after injection, probably due to the shear-thinning properties of mECM hydrogels. Taken together, current decellularization protocol effectively decellularized the meniscus tissue without causing significant loss of ECM main components and possessed porous structure for cell proliferation.

3.2. In vitro studies

3.2.1. BMSCs morphology and viability in mECM

BMSCs were seeded in the decellularized mECM scaffold to evaluate cell viability and ECM synthesis. H&E staining was used to evaluate the distribution of BMSCs in mECM or Cowhide collagen and evaluate the chondrogenic characteristics (Fig. 2). BMSCs showed a high proliferative ability in mECM and Cowhide collagen scaffolds, the number of BMSCs increased significantly over 21 days of culture. Round-shaped chondrocyte-like cells and lacuna structures were distributed homogenously in both mECM and Cowhide collagen groups. Compared with BMSCs-laden Cowhide collagen group, BMSCs-laden mECM group had more chondrocyte-like cells with vacuolated structure. The BMSCs viability in mECM or Cowhide collagen on day 7 was evaluated by LIVE/DEAD® Viability Kit, BMSCs in both gels possess high cell viability (> 90%) which indicates that BMSCs attached and proliferated in both hydrogels (Fig. S1, Supporting Information).

3.2.2. Improved in vitro differentiation of BMSCs using mECM

GAGs is considered to be an important indicator of differentiation towards cartilage. DMMB assay was used to evaluate the impact of mECM on GAGs secretion by BMSCs. As shown in Fig. 3a, the secretion of GAGs increased significantly over time under these two treatments. However, once the GAGs content was normalized to DNA content, we noted the GAGs secretion of mECM + BMSCs group was lower than that of Cowhide collagen + BMSCs group, which was 15.83% less at 21 days ($P < 0.05$).

In order to further evaluate the effect of mECM on fibrocartilaginous differentiation of BMSCs, Toluidine blue and Alcian blue staining (Fig. 3d) were performed to measure the synthesis and secretion of GAGs. Consistent with the H&E staining, cells embedded in Cowhide collagen + BMSCs group secreted less GAGs content than in mECM + BMSCs group. More cells and more intense staining were observed in mECM + BMSCs group than in Cowhide collagen + BMSCs group on day 21. Next, we performed immunohistochemistry staining for collagen I and collagen II. The staining intensity for collagen II in mECM + BMSCs group was higher than that in Cowhide collagen + BMSCs group. Interestingly, mECM also upregulated the expression of collagen I, stronger staining was observed in comparison with Cowhide collagen + BMSCs group. We also extracted the total RNA and proteins of the two groups of cells on day 21 for qRT-PCR and Western blotting to digitally display of the expression of collagen I, collagen II and aggrecan. Fig. 3b indicate that both mECM and Cowhide collagen could effectively induce the expression of fibrocartilage related genes. In horizontal comparison, there is no significant difference between the transcription levels of *collagen II* and *Aggrecan* in mECM + BMSCs and Cowhide collagen + BMSCs groups at 21 days. However, there were significant differences in the expression of *collagen I* between the two groups. mECM was 77.79% higher than that of Cowhide collagen + BMSCs group ($P < 0.05$), which indicates that mECM selectively induced cartilage genes in favor of *Collagen I.* Western blotting results also confirm this observation (Fig. S2, Supporting Information). In addition, we found the cytoskeleton of cells in mECM group exhibited regular alignment pattern, which is similar to the arrangement of fibrin in fibrocartilage (shown in red) (Fig. 3c). However, cytoskeleton in the Cowhide collagen + BMSCs group possessed a disordered pattern. Previous studies have shown that the arrangement of cytoskeleton is essential for the mechanical function of the tissue [25,26].

The morphology and distribution of BMSCs in the scaffolds were observed by SEM (Fig. S3, Supporting Information), which revealed that BMSCs had a flat and adherent morphology and were well attached to the scaffolds, and some cells migrated and attached to interconnecting pores.

3.3. In vivo studies

3.3.1. In vivo subcutaneous implantation of mECM hydrogel

To examine the biocompatibility and chondrogenesis capability of mECM *in vivo*, a heterotopic implantation model was used prior to orthotopic implantation for an initial evaluation. BMSCs seeded within mECM were subcutaneously injected into the back of SD rats after 7 days *in vitro* culture. Histological staining (H&E, Safranin-O and Toluidine blue staining) of the graft was performed after 1 month of post-transplantation (Fig. 4). A large number of cells and strong staining were observed, round-shaped chondrocyte-like cells and lacuna structures were distributed homogenously in mECM.

3.3.2. BMSCs-laden mECM hydrogels promote meniscus regeneration and improve joint function

After two months of implanting BMSCs-laden mECM constructs into orthotopic model of meniscal injury in SD rat, the rats were scarified according to the protocol described in experimental. The general view of the full-thickness defect of meniscus white area is shown in Fig. 5a. In

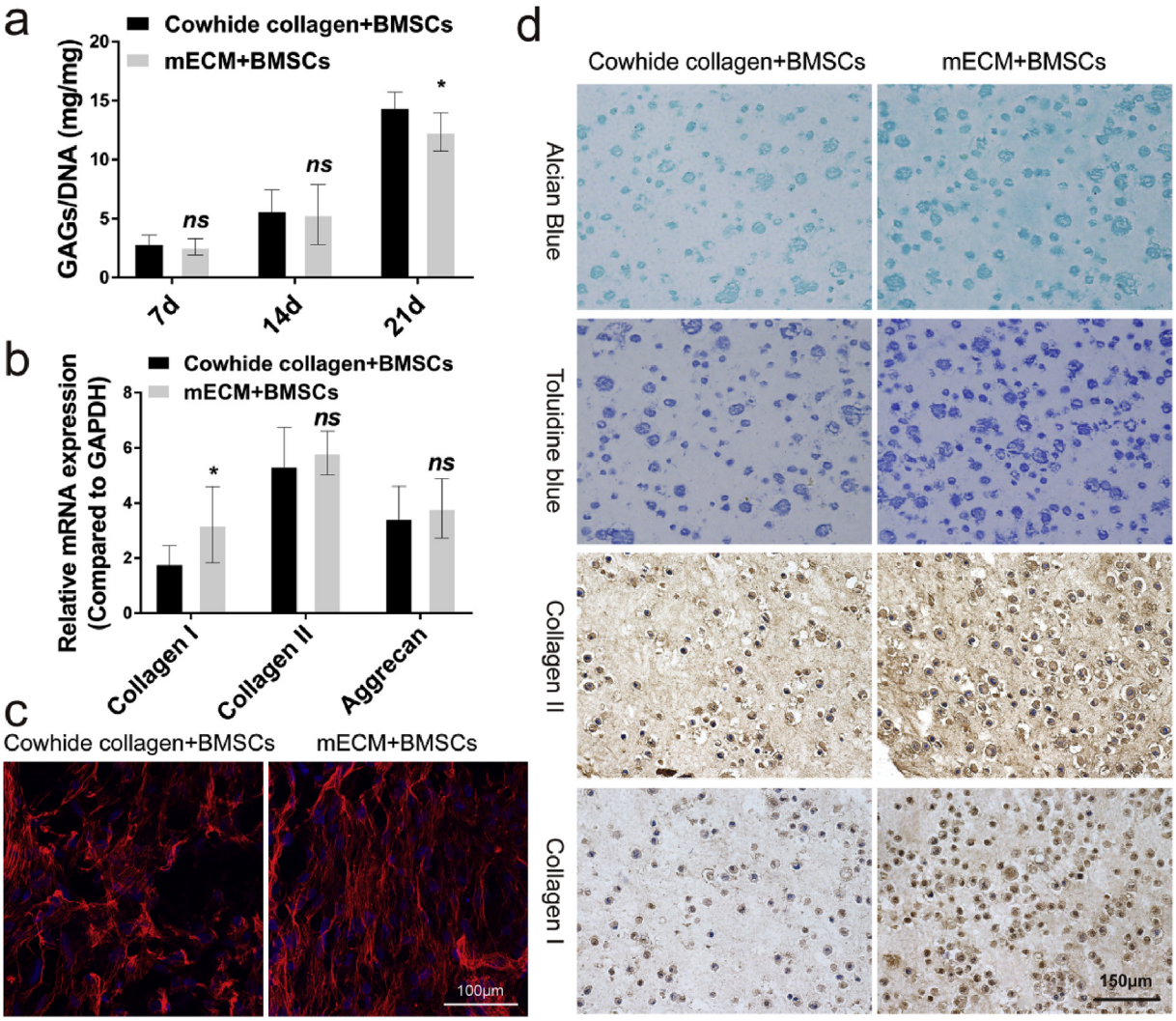

Fig. 3. In vitro fibrochondrogenesis of BMSCs in mECM versus Cowhide collagen. (a) Quantification of matrix production of GAG (n = 6) for cell proliferation. (b) qRT-PCR was used to analyze the gene expression levels of collagen I, collagen II and Aggrecan *in vitro*. (c) Cell skeleton staining of the cells cultured in the mECM or Cowihide collagen for 21 days (scale bar = 100 μm). (d) Alcian blue (top), Toluidine blue, Collagen II and Collagen I (bottom) staining of the cells cultured in the mECM or Cowihide collagen for 21 days (scale bar = 150 μm). Values are presented as means ± SD, n = 6. *, P < 0.05 relative to the normal group.

the control group, the medial meniscus appeared obvious corrosion and wear, which even affected the contralateral meniscus and the whole joint. The tibial plateau also shows characteristics of osteoarthritis like degeneration, which is evidenced in the uneven articular surface and cartilage defects (Fig. 5b).

However, the meniscus and the whole joint of mECM + BMSCs and Cowhide collagen + BMSCs groups maintain a relatively normal structure, shown in the gross appearance of the joints (Fig. 5b). mECM is believed to have capability to facilitate meniscus repair and joint protection. As evidence, the cartilage surface of meniscus and tibial plateau in mECM + BMSC group shows a smoother surface than that of Cowhide collagen + BMSCs group. H&E staining further confirmed our interpretation. H&E staining (Fig. 5c) showed that although Cowhide collagen + BMSCs groups both enhanced the meniscus repair compared to the control group, tissue fibrosis and vascular infiltration can still be observed in the repair area. In contrast, the meniscus repaired by BMSCs-laden mECM group did not show evident pathological characteristics. Safranin O/Fast Green staining revealed the presence of

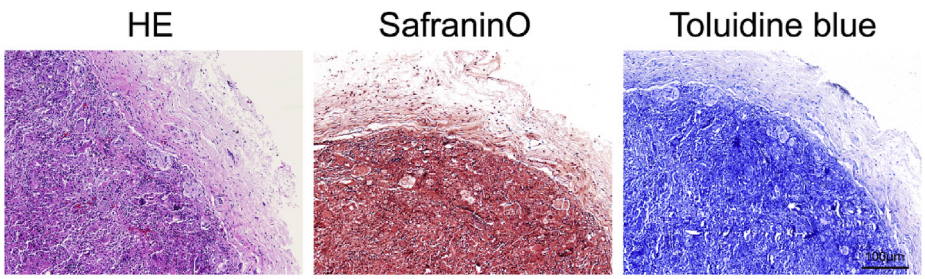

Fig. 4. Evaluation of the effect of mECM on chondrogenesis of BMSCs in a non-cartilage environment by H&E, Safranin-O and Toluidine blue staining after implanted in the back of SD rats for 1 month, scale bar 100 μm n = 6.

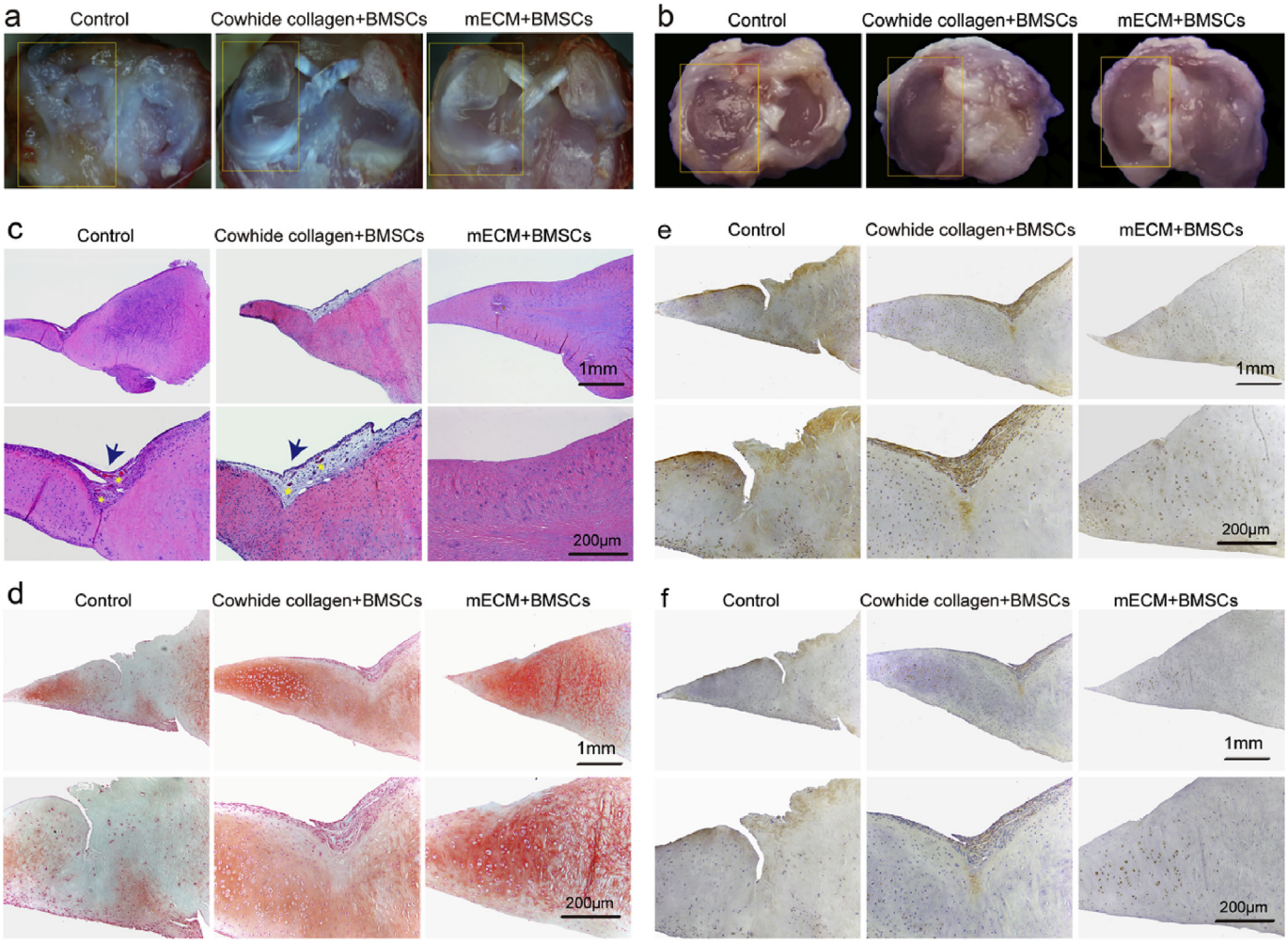

Fig. 5. In vivo meniscus regeneration in defects after implanting BMSCs-seeded mECM scaffolds. (a) Macroscopic appearance of meniscus tissue; (b) Macroscopic appearance of tibial plateau, n = 6; (c)Histological analysis of meniscus regeneration through H&E staining; (d)Safranin O/Fast Green staining; (e)Collagen II and (f)Collagen I staining after two months of treatment with mECM or Cowihide collagen, n = 6. Blue arrows indicate fibrotic tissue; Yellow five-pointed stars indicate blood vessels.

sulfated GAG in hydrogel treated groups, with obviously stronger staining in mECM over Cowhide collagen group (Fig. 5d). mECM and Cowhide collagen treated group had low concentrations of collagen I (Fig. 5f), which is typical for the inner region of the natural meniscus. Surprisingly, although H&E staining shows integrative meniscus repair in mECM treated group, we did not observe a strong straining for markers such as collagen I and collagen II in this group (Fig. 5e).

To investigate whether BMSCs-laden mECM constructs could facilitate meniscus regeneration, protect from joint space narrowing and pathologic mineralization, we carried out micro-CT (μ CT) scanning and reconstruction of the whole lower body of the animal after 1- and 2-months post-transplantation (Fig. 6a). Over time, a large number of hyperosteogeny and osteophyte formation appeared in the control group (PBS treatment only), and the tissue structure of the upper surface of the subchondral bone under the cartilage layer was disordered and uneven. BMSCs-laden hydrogel transplantation effectively decreased the joint degeneration, while mECM was obviously better than Cowhide collagen group in joint protection, mainly because it better maintained the joint bone structure within different treatment time. The joint space volumes (JSV) between the distal femur and proximal tibia, another indicator to show the pathological and healthy state of joint function were quantified by 3D segmentation of CT images. The difference between JSV of left and right knees reflected the joint relaxation and stability (Fig. 6b). In the control group, there was a big volume gap difference between the left and right articular cavities, and the gap difference reached to 33.76 ± 7.38 mm^3 ($p < 0.05$) at two months after transplantation (Fig. 6c). Cell-laden hydrogel significantly reduced the change of articular cavity volume caused by meniscus injury, while BMSCs-laden mECM group had a greater effect in reducing osteophyte formation compared with BMSCs-laden Cowhide collagen group. We further analyzed the μCT images of bone trabecula of femur, as a way to evaluate the preventive effect of BMSCs-laden mECM hydrogel on bone loss caused by meniscus injury (Fig. 6d). We can visually recognize that the mECM + BMSCs has a higher bone density than Cowhide collagen + BMSCs group. The trabeculae in mECM + BMSCs group possessed a denser and more evenly distributed structure. In addition, through quantitative analysis on bone mineral density of trabecula, we found the bone volume/tissue volume (BV/TV) between femoral trabecular and tibial trabecular in mECM + BMSCs group increased by 33.82% and 46.42%, respectively, compared with Cowhide collagen + BMSCs group of identical age and sex at one- and two-months post-transplantation (Fig. 6e). For trabecular number (TB. N), the increase was 20.74% and 18.18%. However, the trabecular bone spacing in the Cowhide collagen + BMSCs was significantly greater than that in the mECM + BMSCs group, and the femoral and tibial plateaus in the collagen group were 62.13% and 18.75% higher than the mECM group, respectively. The trabecular thickness (Tb. Th) of femur and tibia in mECM + BMSCs group was 9.63% and 14.13%

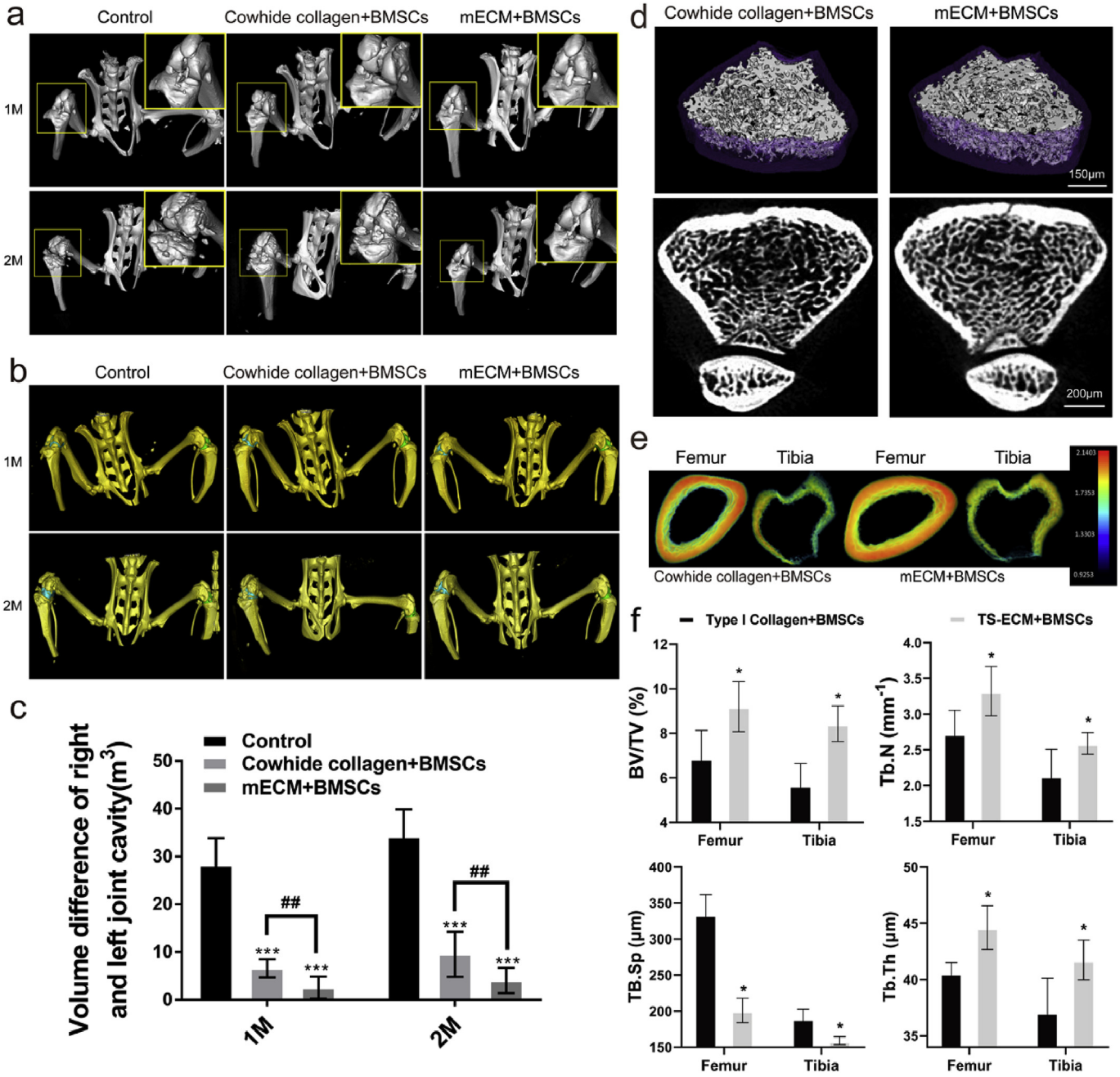

Fig. 6. The effect of mECM on the volume of articular cavity and mineral loss induced by osteoarthritis. (a) Coronal views of 3D reconstruction models of μCT images of joint treated with PBS (Control), BMSCs-laden Cowhide collagen (Cowhide collagen + BMSCs) or BMSCs-laden mECM (mRNA + BMSCs) at 1 and 2 months, n = 3. (b–c) The articular cavity was simulated by three-dimensional reconstruction in rats treated with PBS (Control), BMSCs-laden Cowhide collagen (Cowhide collagen + BMSCs) or BMSCs-laden mECM (mRNA + BMSCs) at 1 and 2 months, n = 3; (d) Femur trabecular bone transection and 3D reconstruction images in rats treated with BMSCs-laden Cowhide collagen (Cowhide collagen + BMSCs) or BMSCs-laden mECM (mRNA + BMSCs) at 2 months, n = 3; (e) Bone mineral density of femoral shaft analyzed by μCT treated with BMSCs-laden Cowhide collagen or BMSCs-laden mECM at 2 months, n = 3; (f) μCT analysis of BV/TV, Tb.N, TB.Sp and Tb.Th obtained from the distal femur after two months of treatment with mECM or Cowihide collagen. n = 3, Values are presented as means ± SD. *, indicates $P < 0.05$; **, $P < 0.01$; ***, $P < 0.001$, relative to the control group. #, $P < 0.05$; ##, $P < 0.01$, relative to the mRNA + BMSCs group.

higher than that in Cowhide collagen + BMSCs group, respectively.

4. Discussion

The overall goal of this study was to prepare an injectable meniscus derived extracellular matrix (mECM) hydrogel to deliver bone marrow stem cells to enhance meniscus repair and regeneration. We show that successful decellularization was achieved based on evaluation of DNA content in decellularized meniscal hydrogel, and confirmed with histological evaluation. There was only a slight decrease in GAGs and collagen content compared to native meniscal tissue after decellularization.

In vitro culture of BMSCs in mECM hydrogel exhibited excellent BMSCs viability, cell proliferation, sulfated GAGs and collagen production superior to cells in Cowhide collagen alone, demonstrating enhanced fibrochondrogenesis of BMSCs observed at days of 7, 14 and 21 *in vitro*. Histology and immunohistochemistry study showed mECM significantly upregulated the expression of collagen I versus of Cowhide

collagen + BMSCs group.

Interestingly, BMSCs in mECM hydrogel exhibited phenotype closer to the natural meniscus cell phenotype. mECM hydrogel not only increased the expression of collagen II and aggrecan, but also upregulated the expression of collagen I. Previous studies have focused on enhancement of collagen II as an indication for regeneration of meniscus, but ignored the important role of collagen I to the contribution of mechanical properties of meniscus, and regarded it as a sign of fibrosis [27]. Previous studies showed that collagen I appeared throughout most of the meniscus, while collagen II was present mainly in the inner meniscus body [28]. The fiber bundles of collagen I is highly organized in parallel arrays. It is this structure that endows meniscus to play important roles in the knee joint, including force transmission, shock absorption in the dynamic load-bearing movement [29]. Collagen II is the main component of hyaline cartilage, which endows hyaline cartilage with the ability to resist the strong compression load [30,31]. As the buffer zone of knee joint, meniscus can maintain the stability of knee joint and relieve the external pressure on knee joint. Therefore, stable collagen I fiber structure plays a significantly role in the maintenance of joint function both under healthy condition and after meniscus injury.

This study indicated that the mECM hydrogel serves two purposes: First, as an ideal vehicle to retain MSCs within the intra-articular environment, providing biochemical cues similar to native meniscus tissue and regulating BMSCs response and formation of fibrocartilage; second, the regenerated fibrocartilage serves to protect from the development of OA, as suggested by the better maintenance of JSV and inhibition of osteoporosis (Fig. 6a, d, e, f). In summary, we demonstrate the use of decellularized porcine meniscus hydrogel (mECM) for intra-articular delivery of rat bone marrow stem cells in an orthotopic rat model of meniscal injury. mECM not only induced the fibrochondrogenesis of encapsulated BMSCs but enhanced integrative meniscus healing and chondroprotection in a SD rat model of meniscus injury.

In the future, extensive studies are required to elucidate the mechanisms of how mECM regulates BMSCs towards chondrogenesis and meniscus repair. In addition, studies are needed to explore the role and mechanism of increased secretion of collagen I in mECM hydrogel for maintenance of knee stability. We are currently focusing on hydrogel development based on ECMs derived from different tissues, both by modifying their mechanical properties and improving hydrogel retention within the intra-articular space for future clinical translation.

CRediT authorship contribution statement

Gang Zhong: Writing - original draft, Data curation, Formal analysis. **Jun Yao:** Writing - original draft. **Xing Huang:** Writing - original draft. **Yixuan Luo:** Writing - original draft. **Meng Wang:** Writing - original draft. **Jinyu Han:** Writing - original draft. **Fei Chen:** Writing - original draft. **Yin Yu:** Writing - original draft.

Declaration of competing interest

The authors declare no conflict of interests.

Acknowledgements

This work was funded by Shenzhen Science and Technology Program (KQTD20170331160605510), Guangxi Natural Science Foundation-Jointly Funded Cultivation Project (2018JJA140982), SIAT Innovation Program for Excellent Young Researcher (Y9G075).

Appendix A. Supplementary data

Supplementary data to this article can be found online at https://doi.org/10.1016/j.bioactmat.2020.06.008.

References

[1] P.S. Walker, M.J. Erkman, The role of the menisci in force transmission across the knee, Clin. Orthop. 109 (1975) 184–192.
[2] S. Kim, J. Bosque, J.P. Meehan, A. Jamali, R. Marder, Increase in outpatient knee arthroscopy in the United States: a comparison of national surveys of ambulatory surgery, 1996 and 2006, J. Bone Jt. Surg. - Ser. A 93 (11) (2011) 994–1000.
[3] A.J.S. Fox, F. Wanivenhaus, A.J. Burge, R.F. Warren, S.A. Rodeo, The human meniscus: a review of anatomy, function, injury, and advances in treatment, Clin. Anat. 28 (2) (2015) 269–287.
[4] S.N. Edd, N.J. Giori, T.P. Andriacchi, The role of inflammation in the initiation of osteoarthritis after meniscal damage, J. Biomech. 48 (8) (2015) 1420–1426.
[5] B. Bilgen, C.T. Jayasuriya, B.D. Owens, Current concepts in meniscus tissue engineering and repair, Adv. Healthc. Mater. 7 (2018) 1701407.
[6] F.A. Monibi, J.L. Cook, Tissue-derived extracellular matrix bioscaffolds: emerging applications in cartilage and meniscus repair, Tissue Eng. B Rev. 23 (4) (2017) 386–398.
[7] F. Qu, F. Guilak, R.L. Mauck, Cell migration: implications for repair and regeneration in joint disease, Nat. Rev. Rheumatol. 15 (2019) 167–179.
[8] Z.Z. Zhang, D. Jiang, J.X. Ding, S.J. Wang, L. Zhang, J.Y. Zhang, Y.S. Qi, X.S. Chen, J.K. Yu, Role of scaffold mean pore size in meniscus regeneration, Acta Biomater. 43 (2016) 314–326.
[9] X. Yuan, Y. Wei, A. Villasante, J.J.D. Ng, D.E. Arkonac, P. Chao, G. hsiu, G. Vunjak-Novakovic, Stem cell delivery in tissue-specific hydrogel enabled meniscal repair in an orthotopic rat model, Biomaterials 132 (2017) 59–71.
[10] Y. Moriguchi, K. Tateishi, W. Ando, K. Shimomura, Y. Yonetani, Y. Tanaka, K. Kita, D.A. Hart, A. Gobbi, K. Shino, et al., Repair of meniscal lesions using a scaffold-free tissue-engineered construct derived from allogenic synovial MSCs in a miniature swine model, Biomaterials 34 (2013) 2185–2193.
[11] Z. Pan, Y. Wu, X. Zhang, Q. Fu, J. Li, Y. Yang, D. Yu, Y. Xu, X. Lu, H. Sun, et al., Delivery of epidermal growth factor receptor inhibitor via a customized collagen scaffold promotes meniscal defect regeneration in a rabbit model, Acta Biomater. 62 (2017) 210–221.
[12] Y. Liang, E. Idrees, A.R.A. Szojka, S.H.J. Andrews, M. Kunze, A. Mulet-Sierra, N.M. Jomha, A.B. Adesida, Chondrogenic differentiation of synovial fluid mesenchymal stem cells on human meniscus-derived decellularized matrix requires exogenous growth factors, Acta Biomater. 80 (2018) 131–143.
[13] J. Wua, Q. Ding, A. Dutta, Y. Wang, Y.H. Huang, H. Wenga, L. Tang, Y. Hong, An injectable extracellular matrix derived hydrogel for meniscus repair and regeneration, Acta Biomater. 16 (1) (2015) 49–59.
[14] A.L. McNulty, L.P. Lyons, S.H. Perea, J.B. Weinberg, J.R. Wittstein, Meniscus-derived matrix bioscaffolds: effects of concentration and cross-linking on meniscus cellular responses and tissue repair, Int. J. Mol. Sci. 21 (1) (2020) 44.
[15] J.C. Ruprecht, T.D. Waanders, C.R. Rowland, J.F. Nishimuta, K.A. Glass, J. Stencel, L.E. DeFrate, F. Guilak, J.B. Weinberg, A.L. McNulty, Meniscus-derived matrix scaffolds promote the integrative repair of meniscal defects, Sci. Rep. 9 (1) (2019) 8719.
[16] D.C. Browe, O.R. Mahon, P.J. Díaz-Payno, N. Cassidy, I. Dudurych, A. Dunne, C.T. Buckley, D.J. Kelly, Glyoxal cross-linking of solubilized extracellular matrix to produce highly porous, elastic, and chondro-permissive scaffolds for orthopedic tissue engineering, J. Biomed. Mater. Res. 107 (10) (2019) 2222–2234.
[17] F.A. Monibi, C.C. Bozynski, K. Kuroki, A.M. Stoker, F.M. Pfeiffer, S.L. Sherman, J.L. Cook, Development of a micronized meniscus extracellular matrix scaffold for potential augmentation of meniscal repair and regeneration, Tissue Eng. C Methods 22 (12) (2016) 1059–1070.
[18] T.W. Stapleton, J. Ingram, J. Katta, R. Knight, S. Korossis, J. Fisher, E. Ingham, Development and characterization of an acellular porcine medial meniscus for use in tissue engineering, Tissue Eng. 14 (4) (2008) 505–518.
[19] G.K. Reddy, C.S. Enwemeka, A simplified method for the analysis of hydroxyproline in biological tissues, Clin. Biochem. 29 (3) (1996) 225–229.
[20] R.W. Farndale, D.J. Buttle, A.J. Barrett, Improved quantitation and discrimination of sulphated glycosaminoglycans by use of dimethylmethylene blue, Biochim. Biophys. Acta 883 (1986) 173–177.
[21] J. Li, N. Ren, J. Qiu, H. Jiang, H. Zhao, G. Wang, R.I. Boughton, Y. Wang, H. Liu, Carbodiimide crosslinked collagen from porcine dermal matrix for high-strength tissue engineering scaffold, Int. J. Biol. Macromol. 61 (2013) 69–74.
[22] T.D. Bornes, N.M. Jomha, A. Mulet-Sierra, A.B. Adesida, Hypoxic culture of bone marrow-derived mesenchymal stromal stem cells differentially enhances in vitro chondrogenesis within cell-seeded collagen and hyaluronic acid porous scaffolds, Stem Cell Res. Ther. 6 (1) (2015) 84.
[23] N.Y. Ignat'eva, N.A. Danilov, S.V. Averkiev, M.V. Obrezkova, V.V. Lunin, E.N. Sobol', Determination of hydroxyproline in tissues and the evaluation of the collagen content of the tissues, J. Anal. Chem. 62 (1) (2007) 51–57.
[24] T. Aigner, K.R. Greskötter, J.C.T. Fairbank, K. Von Der Mark, J.P.G. Urban, Variation with age in the pattern of type X collagen expression in normal and scoliotic human intervertebral discs, Calcif. Tissue Int. 63 (3) (1998) 263–268.
[25] D.A. Fletcher, R.D. Mullins, Cell mechanics and the cytoskeleton, Nature 463 (7280) (2010) 485–492.
[26] Q. Li, F. Qu, B. Han, C. Wang, H. Li, R.L. Mauck, L. Han, Micromechanical anisotropy and heterogeneity of the meniscus extracellular matrix, Acta Biomater. 54 (2017) 356–366.
[27] Y. Chen, J. Chen, Z. Zhang, K. Lou, Q. Zhang, S. Wang, J. Ni, W. Liu, S. Fan, X. Lin, Current advances in the development of natural meniscus scaffolds: innovative approaches to decellularization and recellularization, Cell Tissue Res. 370 (2017) 41–52.

[28] Y. Sun, Histological examination of collagen and proteoglycan changes in osteoarthritic menisci, Open Rheumatol. J. 6 (1) (2012) 24–32.
[29] A.J. Freemont, J. Hoyland, Lineage plasticity and cell biology of fibrocartilage and hyaline cartilage: its significance in cartilage repair and replacement, Eur. J. Radiol. 57 (1) (2006) 32–36.
[30] M. Freutel, H. Schmidt, L. Dürselen, A. Ignatius, F. Galbusera, Finite element modeling of soft tissues: material models, tissue interaction and challenges, Clin. Biomech. 29 (4) (2014) 363–372.
[31] E.M. Hasler, W. Herzog, J.Z. Wu, W. Müller, U. Wyss, Articular cartilage biomechanics: theoretical models, material properties, and biosynthetic response, Crit. Rev. Biomed. Eng. 27 (6) (1999) 415–488.